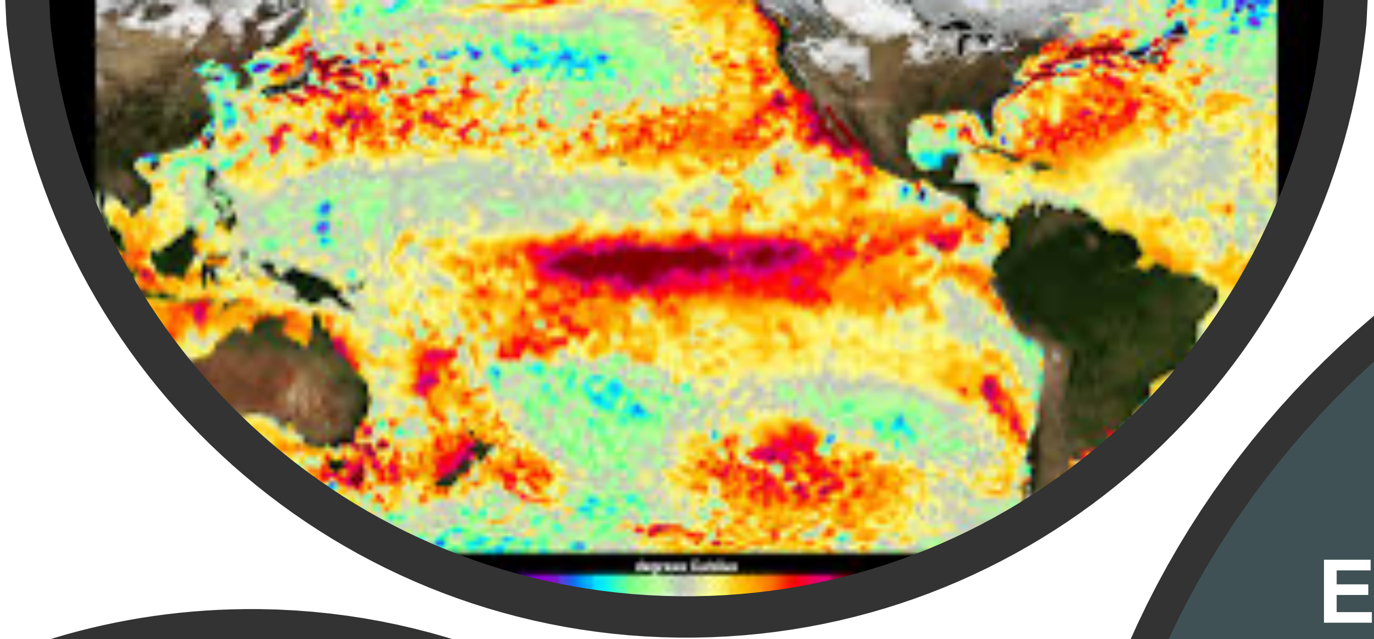

Exploring the manifold of the tropical Pacific in observations and models

Fabrizio Falasca – Annalisa Bracco

arXiv:2110.03614v1

Why the tropical Pacific?

Annual Mean Sea Surface Temperature (SST)

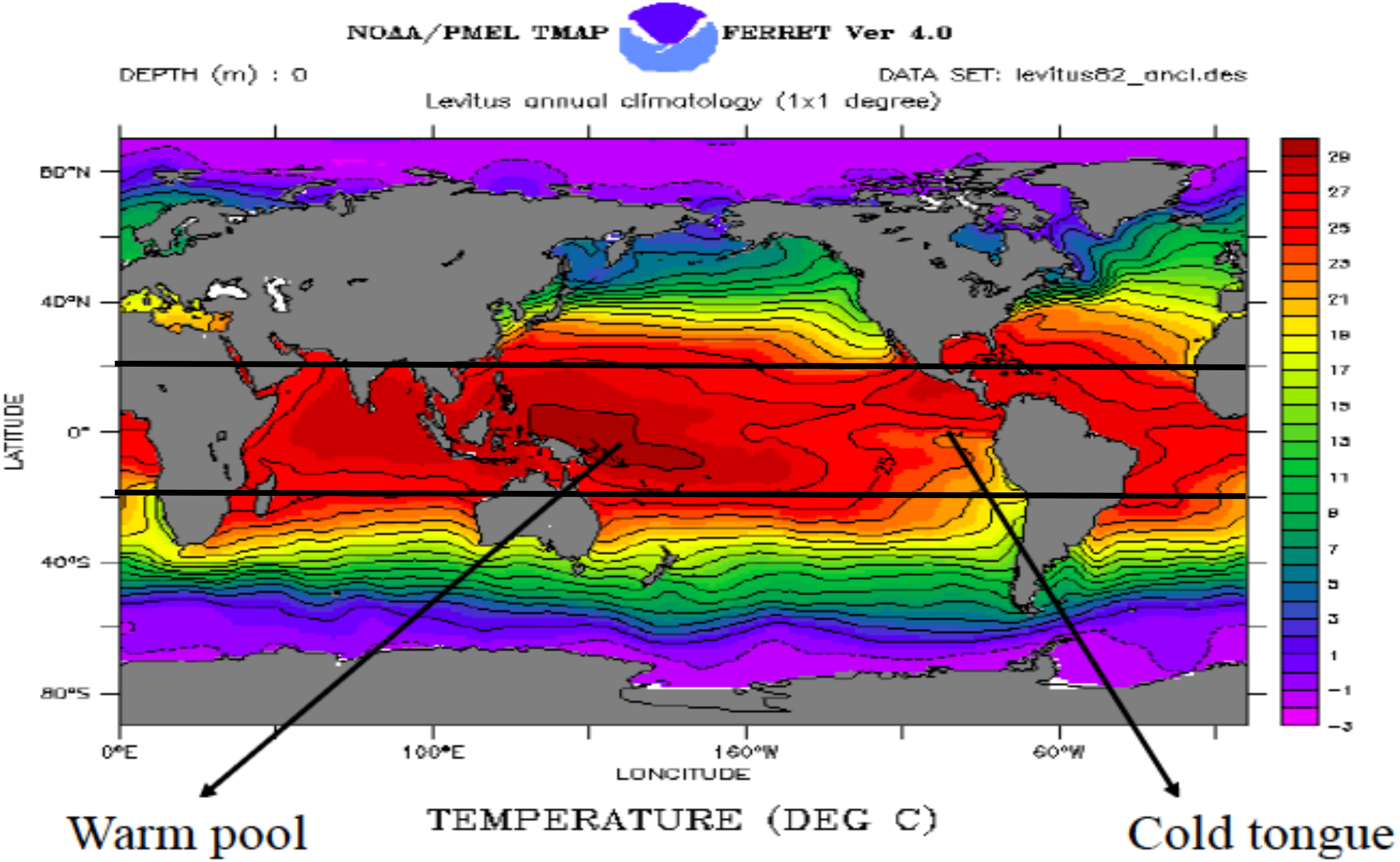

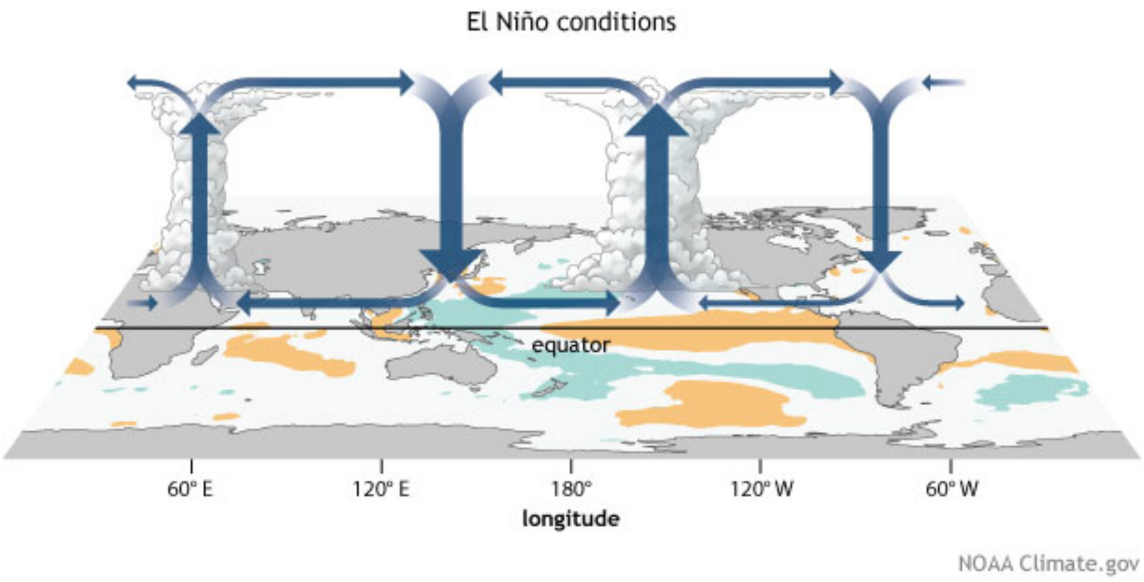
El Niño conditions
equator
60° E
120° E
180°
120° W
60° W
longitude
NOAA Climate.gov

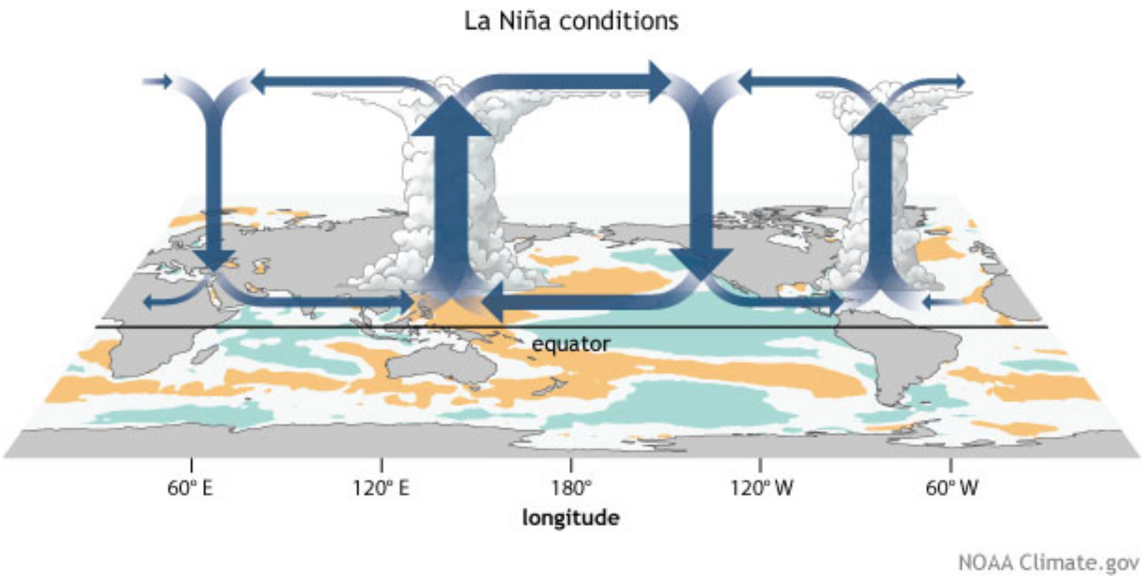
La Niña conditions
equator
60° E
120° E
180°
120° W
60° W
longitude
NOAA Climate.gov

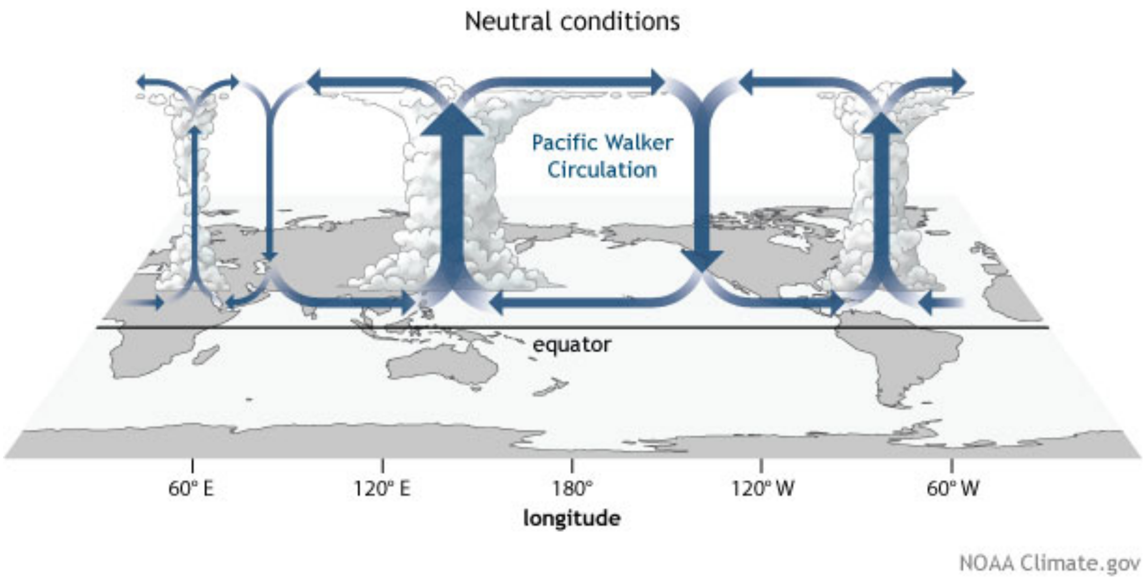
Neutral conditions
Pacific Walker
Circulation
equator
60° E
120° E
180°
120° W
60° W
longitude
NOAA Climate.gov

ENSO

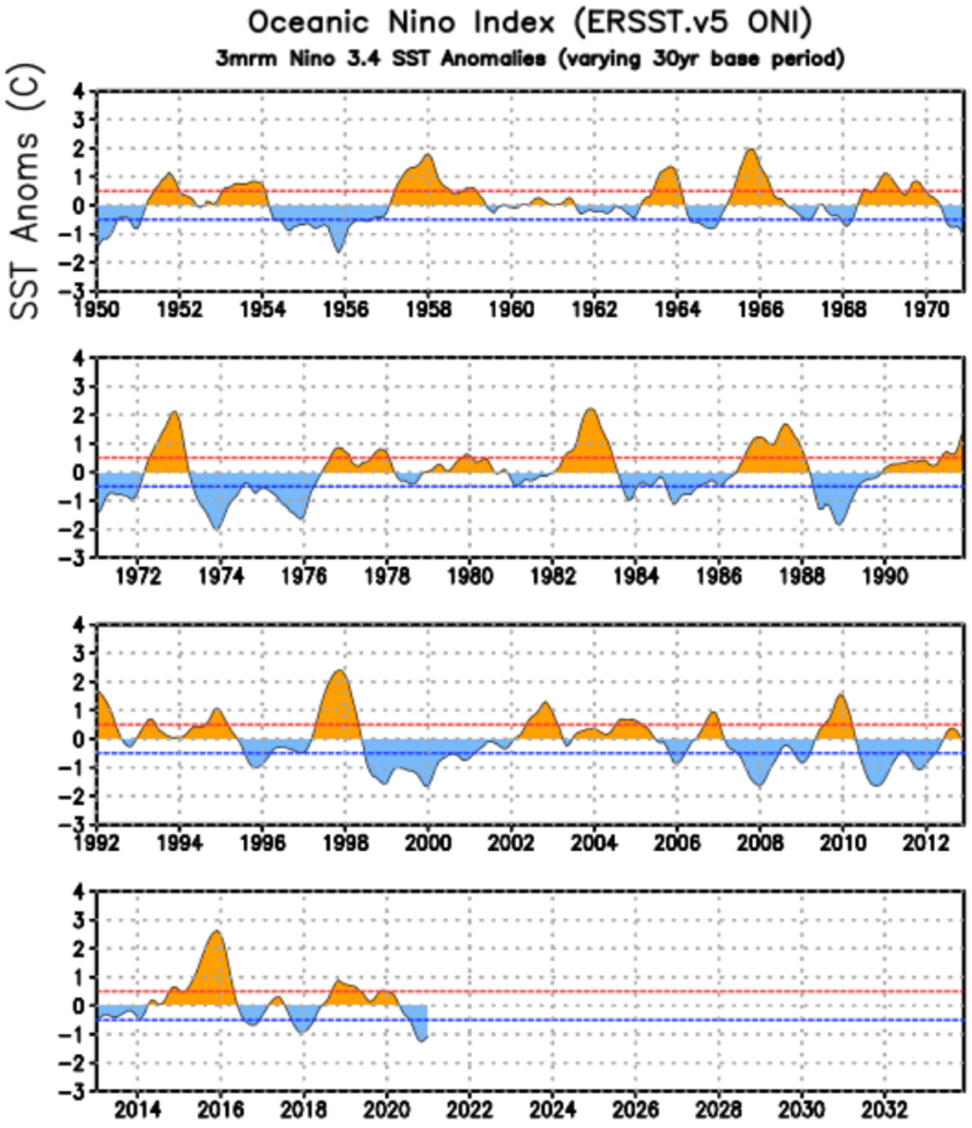

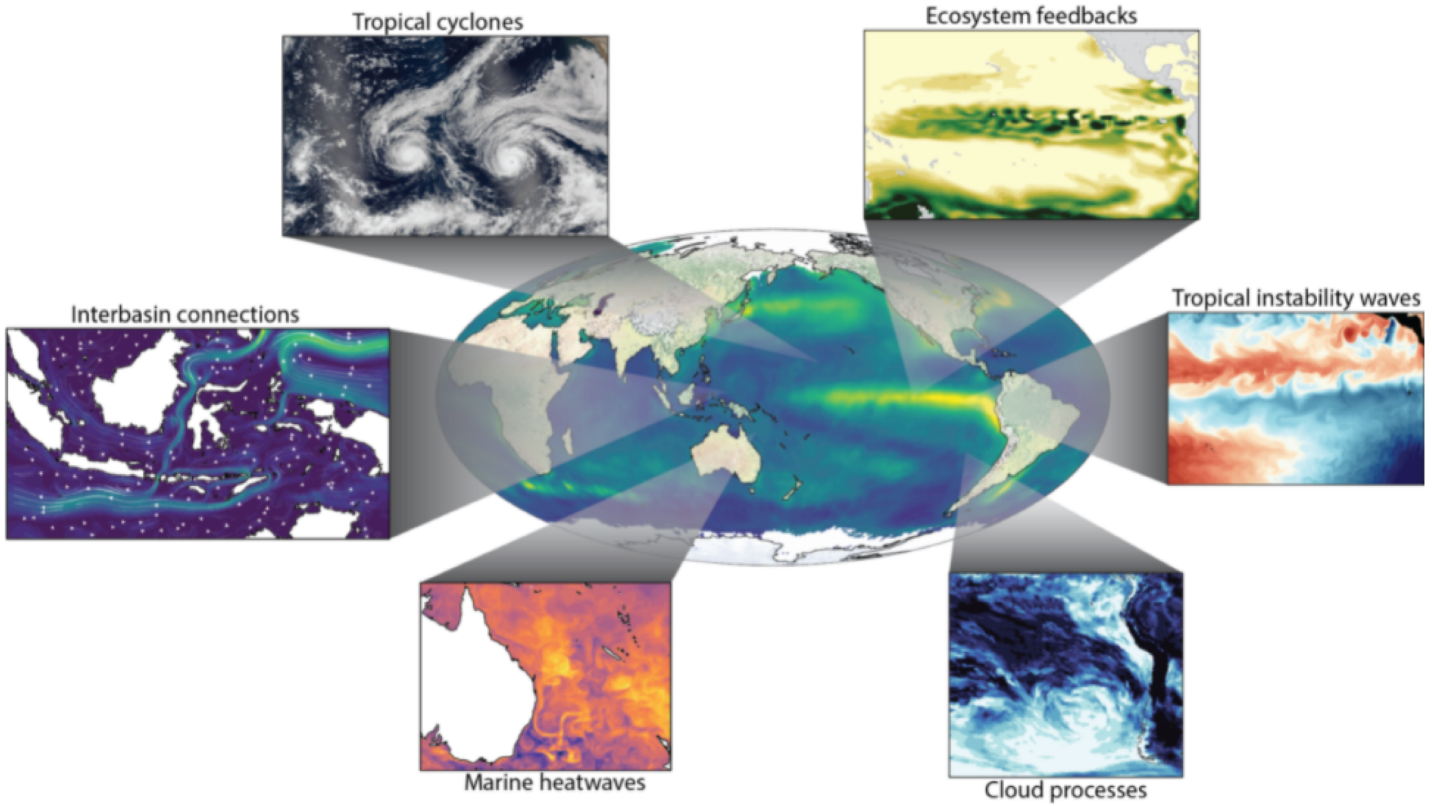

Karamperidou et al. (2020)

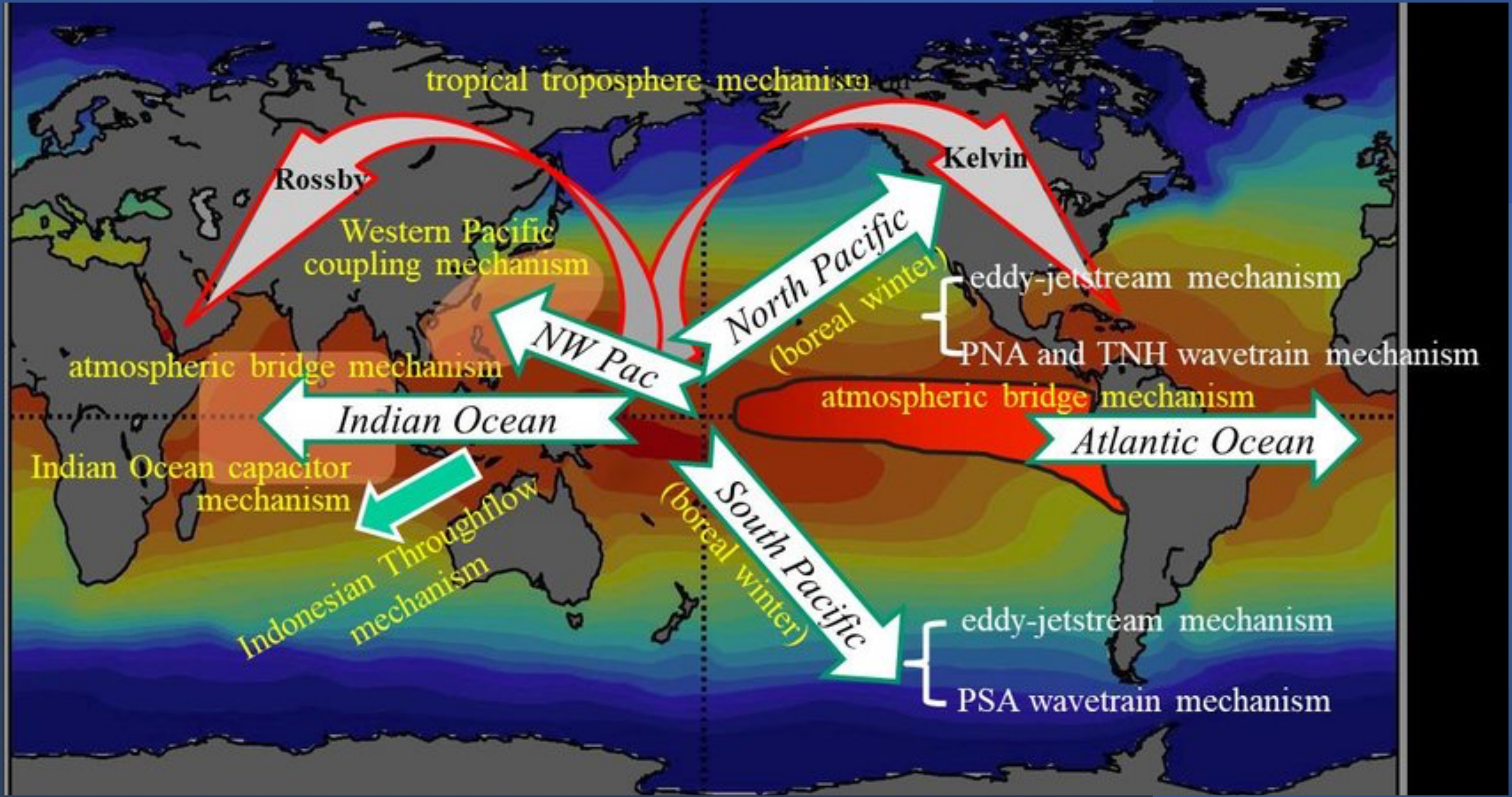
tropical troposphere mechanism
Rossby
Kelvin
Western Pacific coupling mechanism
NW Pac
North Pacific
(boreal winter)
eddy-jetstream mechanism
PNA and TNH wavetrain mechanism
atmospheric bridge mechanism
Indian Ocean
atmospheric bridge mechanism
Atlantic Ocean
Indian Ocean capacitor mechanism
Indonesian Throughflow mechanism
(boreal winter)
South Pacific
eddy-jetstream mechanism
PSA wavetrain mechanism

ENSO in the future

Article | Published: 26 August 2021

Future high-resolution El Niño/Southern Oscillation dynamics

Christian Wengel, Sun-Seon Lee, Malte F. Stuecker, Axel Timmermann, Jung-Eun Chu & Fabian Schloesser

Here, using a mesoscale-resolving global climate model with an improved representation of tropical climate, we show that a **quadrupling of atmospheric CO_2 causes a robust weakening of future simulated ENSO sea surface temperature variability**.

Geophysical Research Letters

Research Letter | Open Access

How Does El Niño–Southern Oscillation Change Under Global Warming—A First Look at CMIP6

Hege-Beate Fredriksen, Judith Berner, Aneesh C. Subramanian, Antonietta Capotondi,

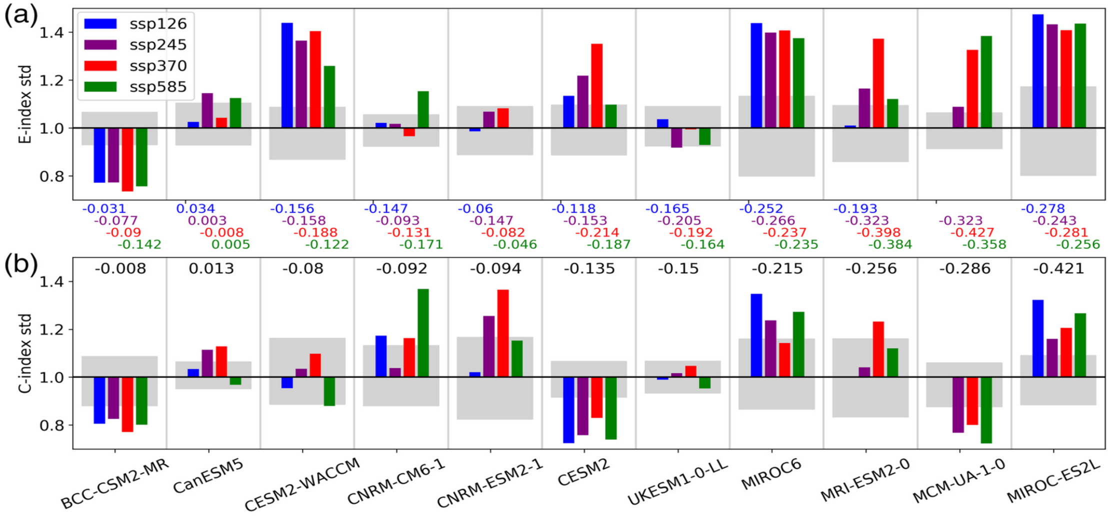

Geophysical Research Letters, Volume: 47, Issue: 22, First published: 22 October 2020, DOI: (10.1029/2020GL090640)

August 2020 **NOAA RESEARCH NEWS**

"**Extreme El Niño and La Niña events may increase in frequency from about one every 20 years to one every 10 years by the end of the 21st** century under aggressive greenhouse gas emission scenarios," McPhaden said. "**The strongest events may also become even stronger** than they are today."

Challenges in climate science

- The climate system is **multiscale, multidimensional and nonlinear**
- Very large number of variables
- Limited observations, especially before satellites
- Not all equations are known (think aerosols+clouds interactions)

Something helpful

The climate system is a high-dimensional, nonlinear and dissipative (Lucarini, 2016).

Its dynamics is expected to be confined to a manifold with lower dimension than the full state space

Dimensionality reduction is traditionally performed via Principal Component Analysis (PCA) or Empirical Orthogonal Functions (EOF) but we now have better tools that account for nonlinearities

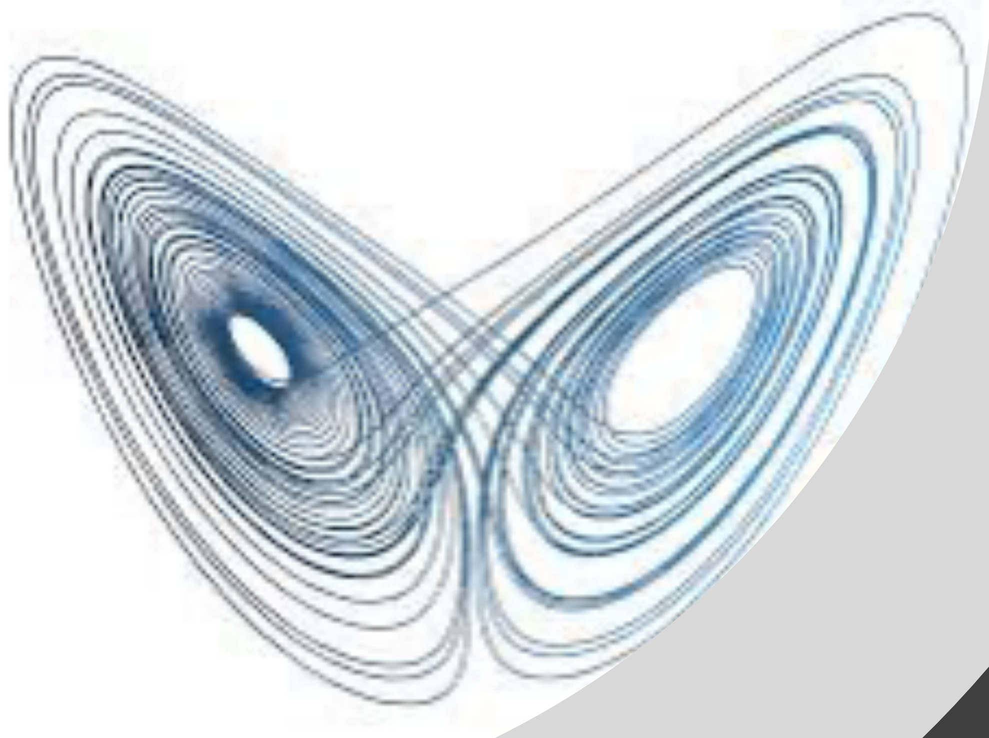

GOAL

A **nonlinear, multivariable, dimensional reduction framework** for climate science based on manifold characterization (here applied to the tropical Pacific)

DATA

ERA5 (reanalysis), two CMIP6 (newest generation) climate models: MPI and EC-Earth (high resolution)

1979-2019 reanalysis and models, and 2060-2100 models under the SSP585 scenario. Daily data

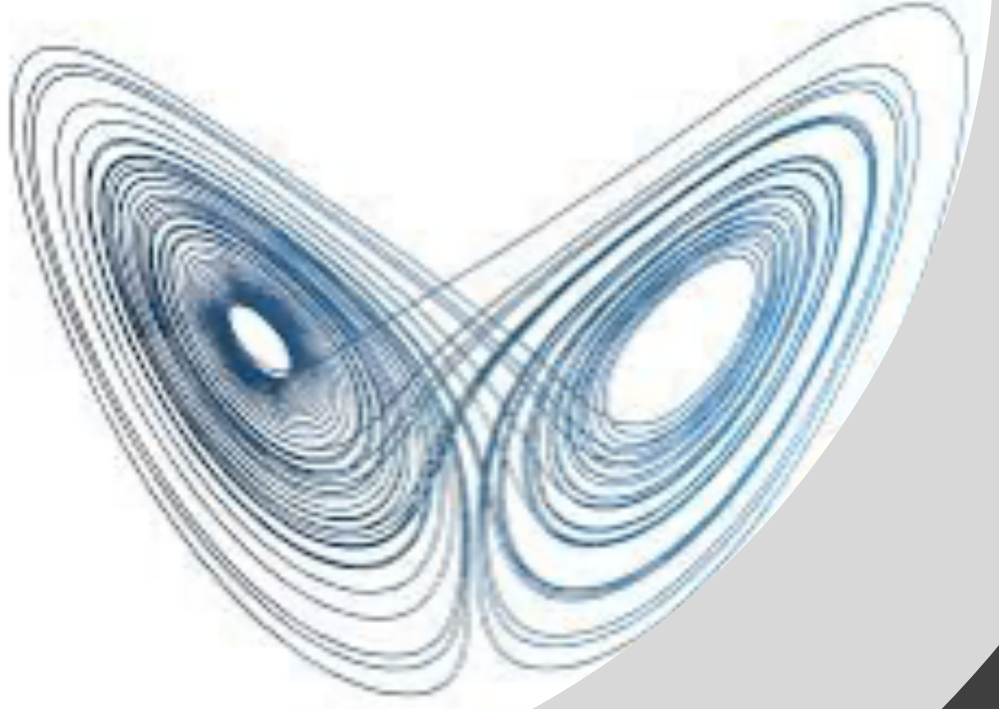

MPI: MPI-ESM1.2-HR

Atmos: ECHAM6.3 $1^o x 1^o$, 95 vertical levels

Ocean: MPIOM1.63 $0.4^o x 0.4o$, 40 levels

Land: JSBACK3.20 No dynamical vegetation, carbon and nitrogen cycles

Ocean biogeochem: HAMOCC

EC-EARTH: EC-Earth3-HR

Atmosphere and Land: ECMWF's IFS 125 cycle 36r4 T511 spectral resolution for IFS

Ocean and Ice: NEMO3.6 and LIM3 $0.25^o x 0.25^o$ resolution

Ocean Biogeochem: PISCES model.

Dynamical vegetation, land use and terrestrial biogeochemistry: LPJ-GUESS.

Atmos chem: TM5

https://gmd.copernicus.org/preprints/gmd-2020-446/gmd-2020-446.pdf

Steps

Select a **subset N of representative variables** (here SST, near-surface winds u and v, outgoing longwave radiation OLR) defining a high dimensional trajectory **X**(t)$\in \mathbb{R}^{T,N}$ (N = 17,092-dimensional trajectory in our case, T~14,000)

Identify the intrinsic manifolds both with a linear (PCA) and a **nonlinear (Isomap)** dimensionality reduction method

PCA identifies the manifold by fitting hyperplanes in the directions that contain most of the variance; Isomap first identifies the K-nearest neighbors of each point i in the manifold and then computes the geodesic distances δ(i,j) between each couple of points i, j assuming that the manifold is locally flat in a radius of K points (here 10)

Estimate local geometry and stability of the attractor through its **local dimension *d*(ζ)** metric and the **inverse of the average persistence** of the trajectory around ζ, where ζ=**X**(τ) with τ ∈ [1,T]. *d*(ζ) ~ number of directions the system can evolve from/into. **θ(ζ)** ~ stickiness of the trajectory around ζ (Faranda et al., *Sci*. *Rep*., 2017)

Metrics: Local Dimension

Requiring that the orbit falls into a neighborhood of the point ζ is equivalent to asking that the time series $g(\boldsymbol{x}(t), \zeta)$ exceeds a threshold $s(q, \zeta)$

Extremes and Recurrence in Dynamical system
V. Lucarini et al. Wiley, New York, 2016

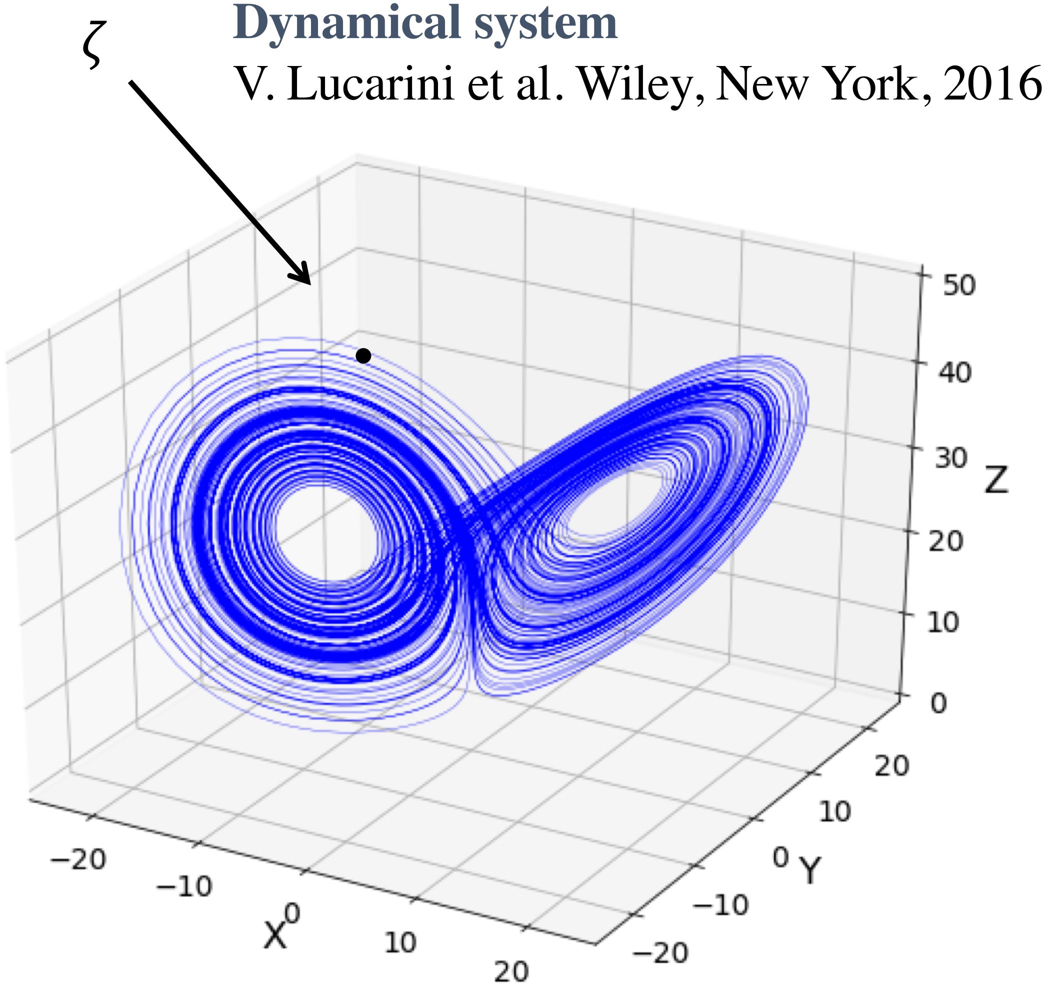

Freitas-Freitas-Todd Theorem

$$P(g(\boldsymbol{x}(t), \zeta) > s(q, \zeta)) \sim \exp(-\frac{u(\zeta)}{\sigma(\zeta)})$$

With $u(\zeta) = g(\boldsymbol{x}(t), \zeta) - s(q, \zeta)$ and q being a high quantile from the time series $g(\boldsymbol{x}(t), \zeta)$

$$d(\zeta) = 1 / \sigma(\zeta)$$

Theorem proved for chaotic systems.

Extremes and Recurrence in Dynamical system

V. Lucarini et al. Wiley, New York, 2016

$d(\zeta)$

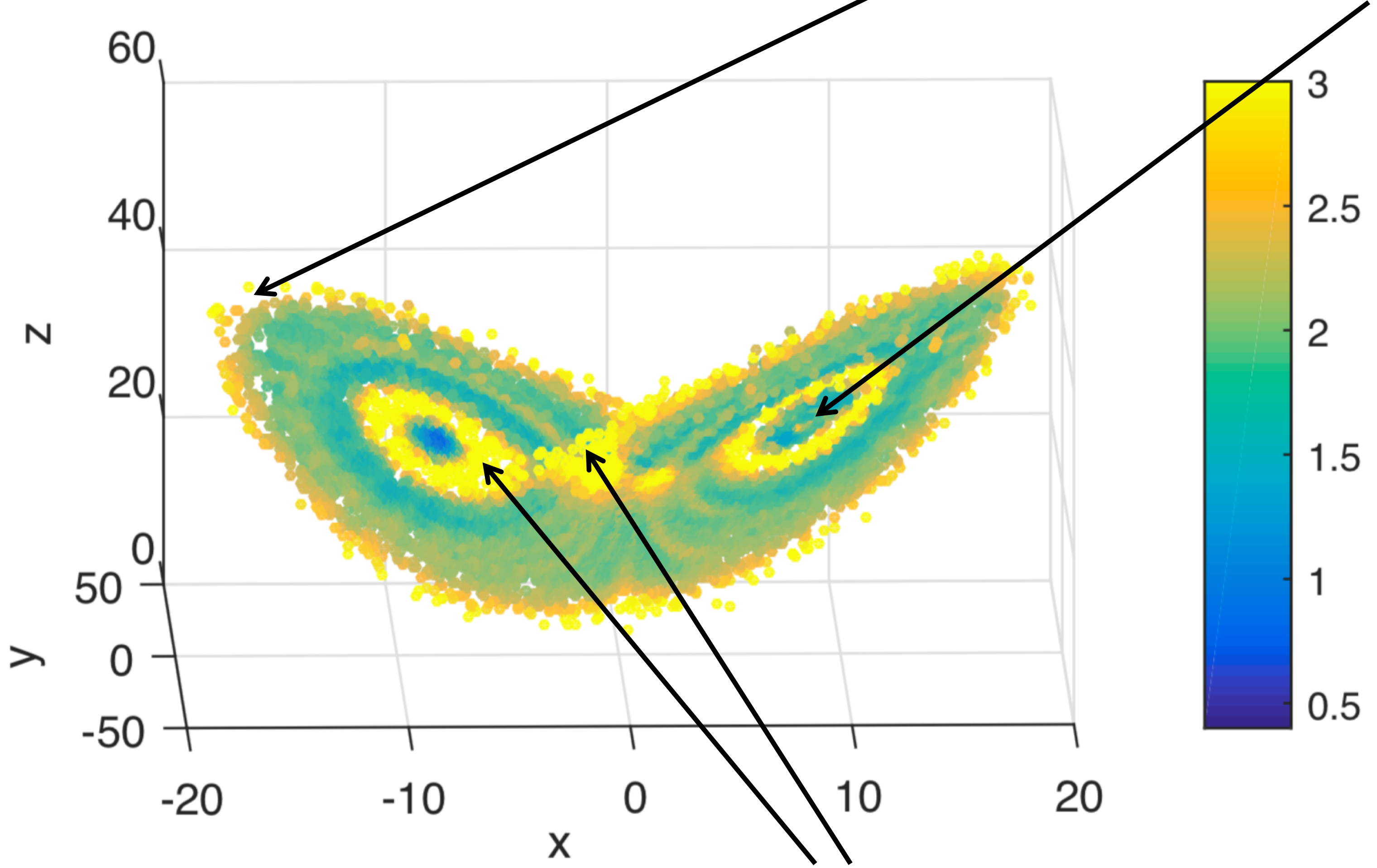

Higher dimension because few episodes (reflects uncertainty)

Lower dimension closer to fixed points

Average dimension:

D= <d> = 2.06

Divergence of trajectory: higher dimension

Metrics: Persistence or local stability

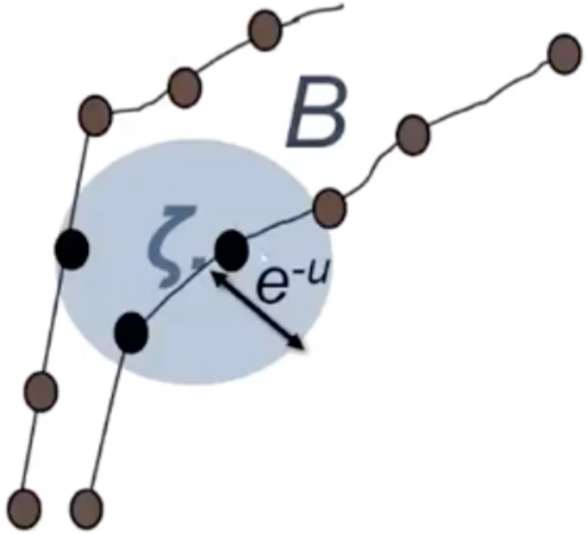

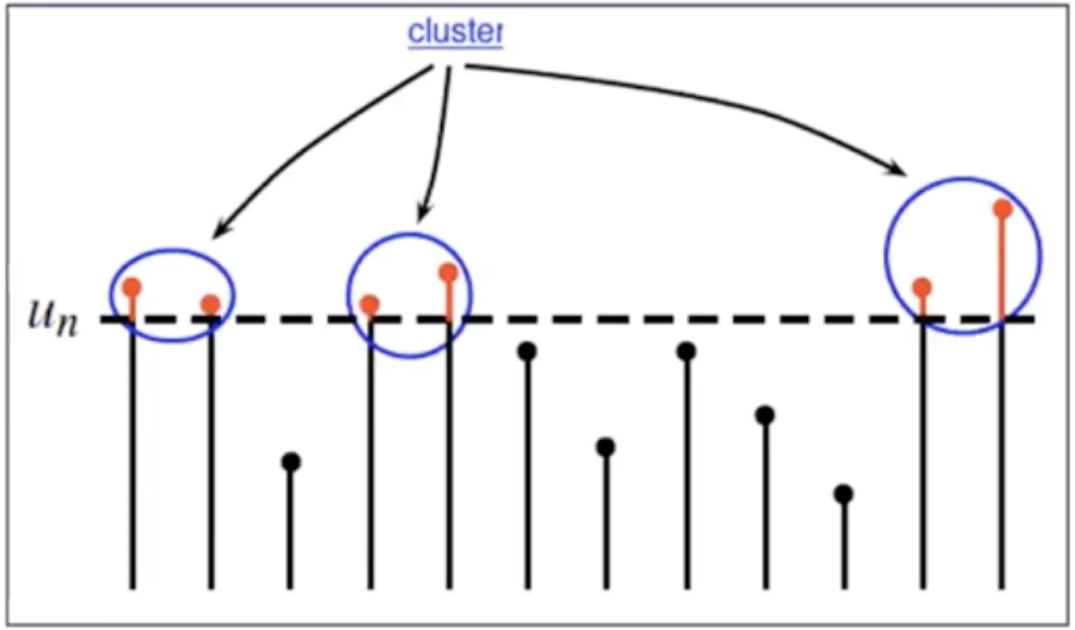

Points inside a neighborhood of ζ ←→ points that exceed a (high) threshold u in the observable g

Inverse of persistency ϑ **:** can be thought as the inverse of the average time spent above u

$\vartheta(\zeta)$

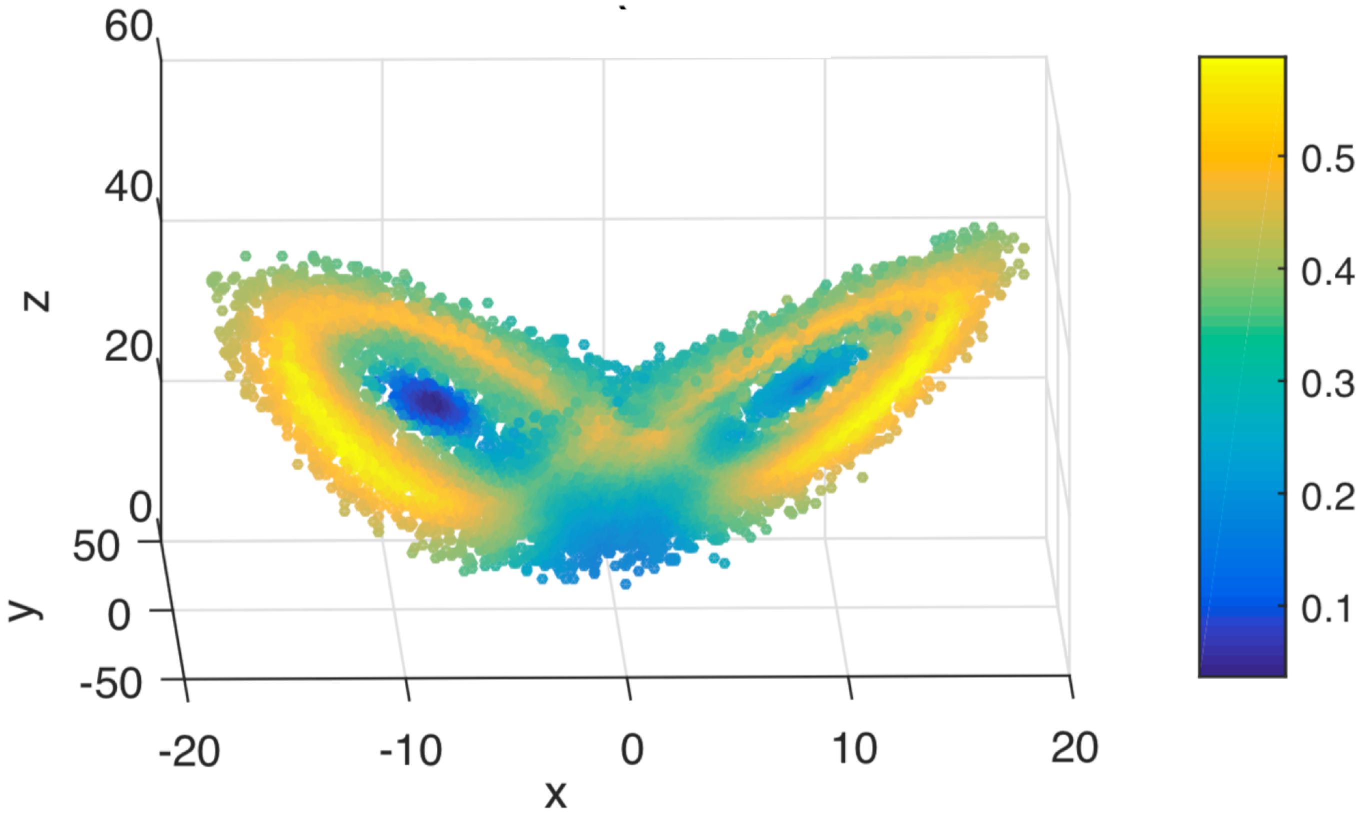

ϑ: good proxy for unstable fixed points of the system

Quantifies stability of points in state space

Results: Seasonal cycle

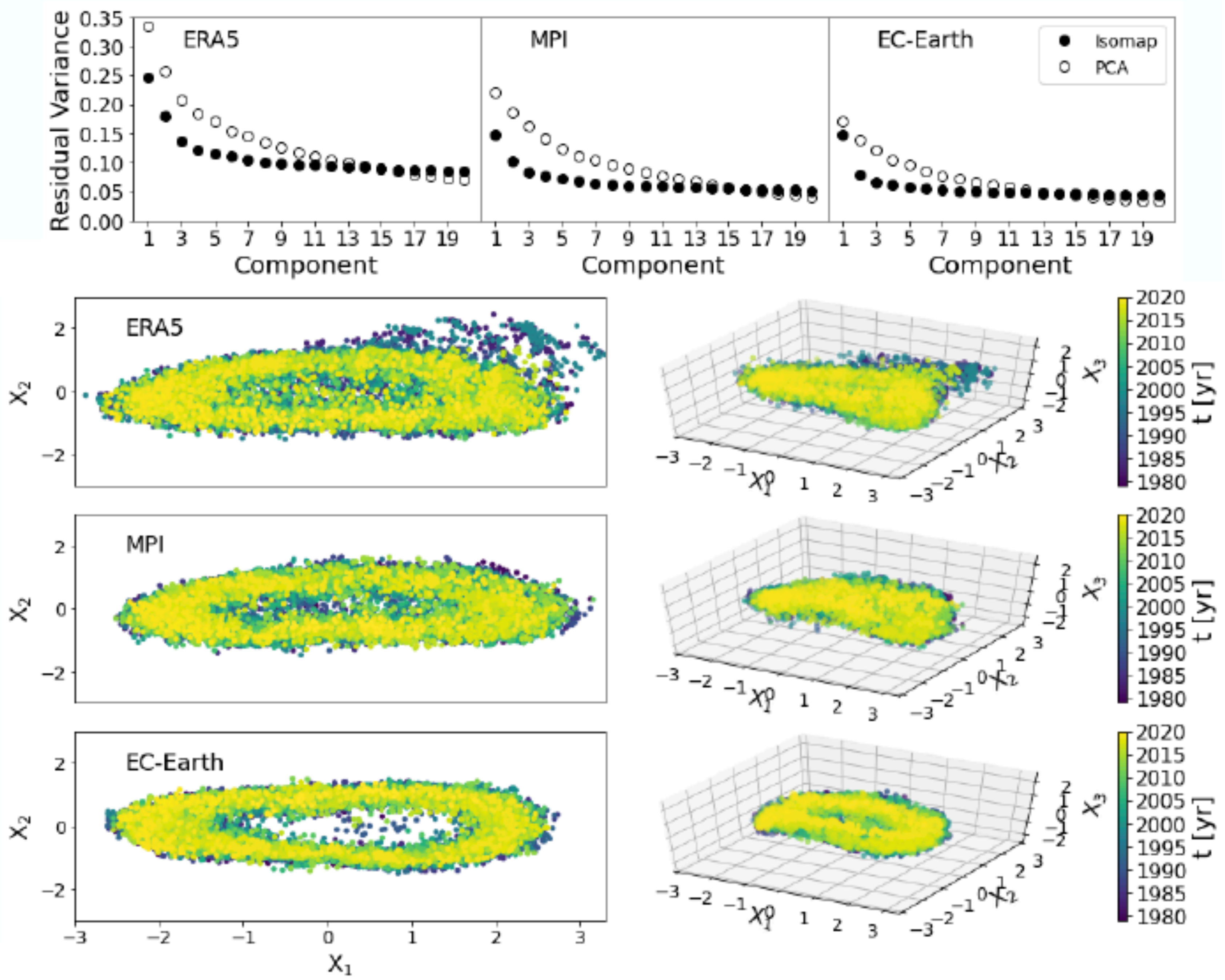

Results: Seasonal cycle

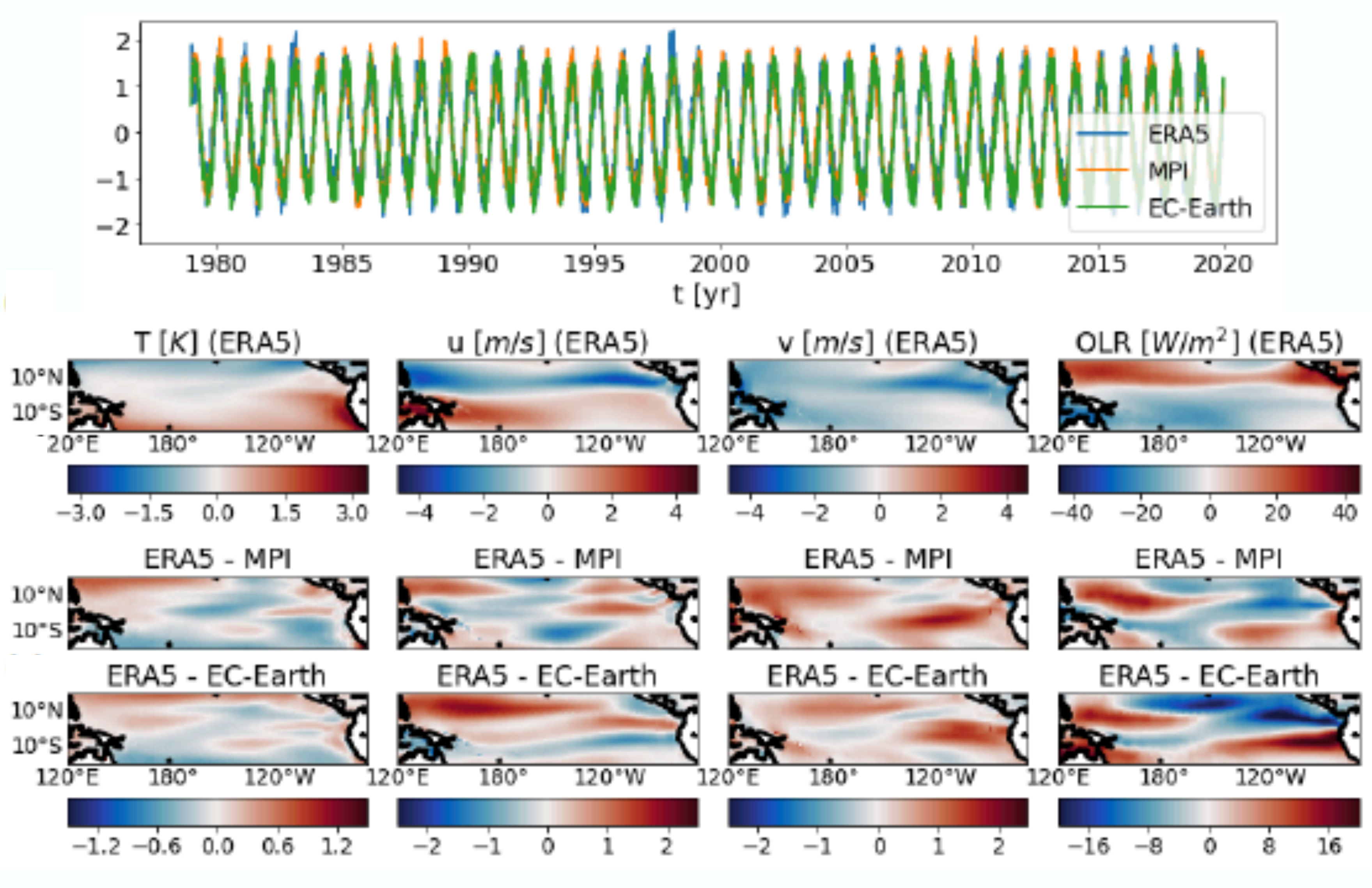

Results: ENSO variability

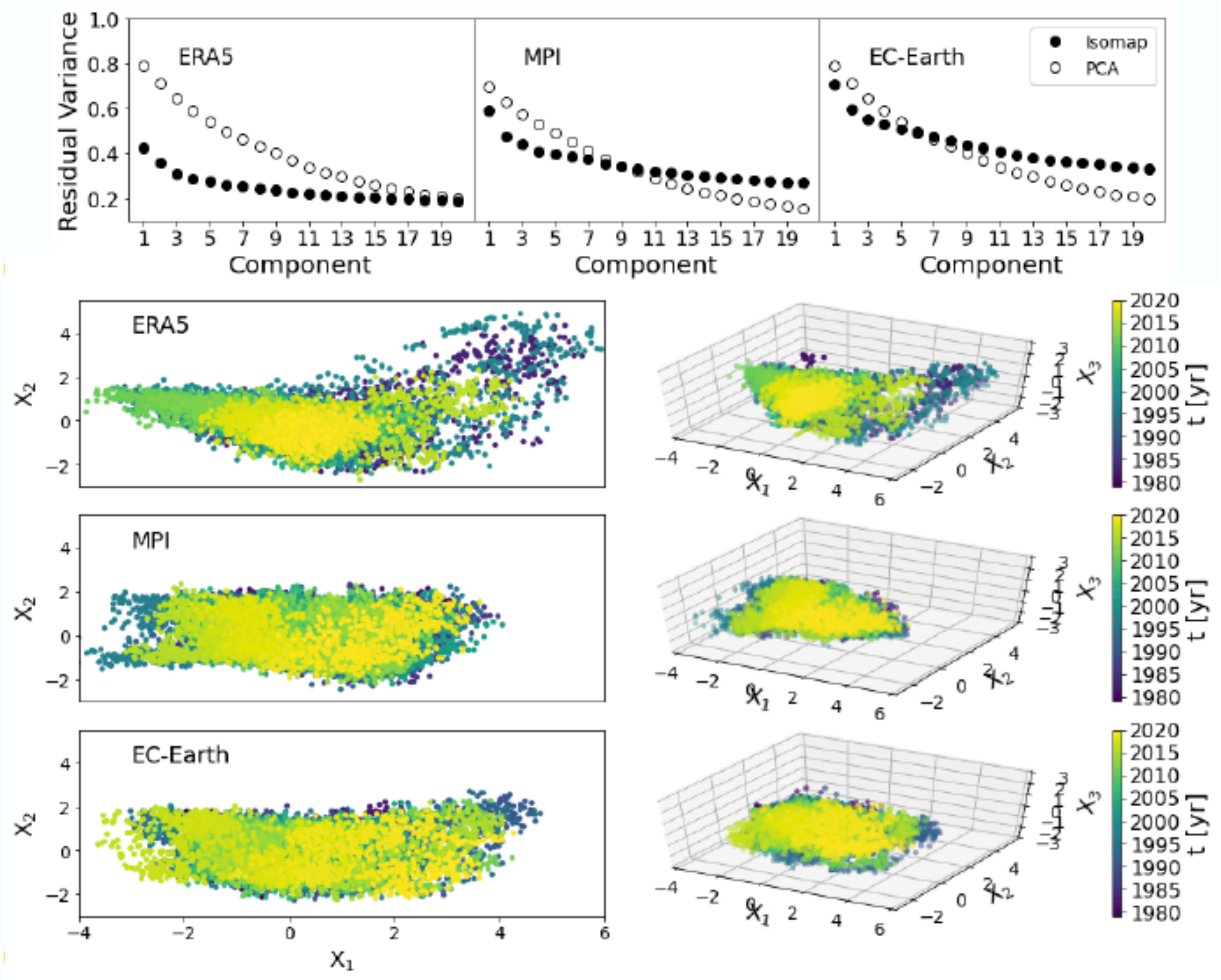

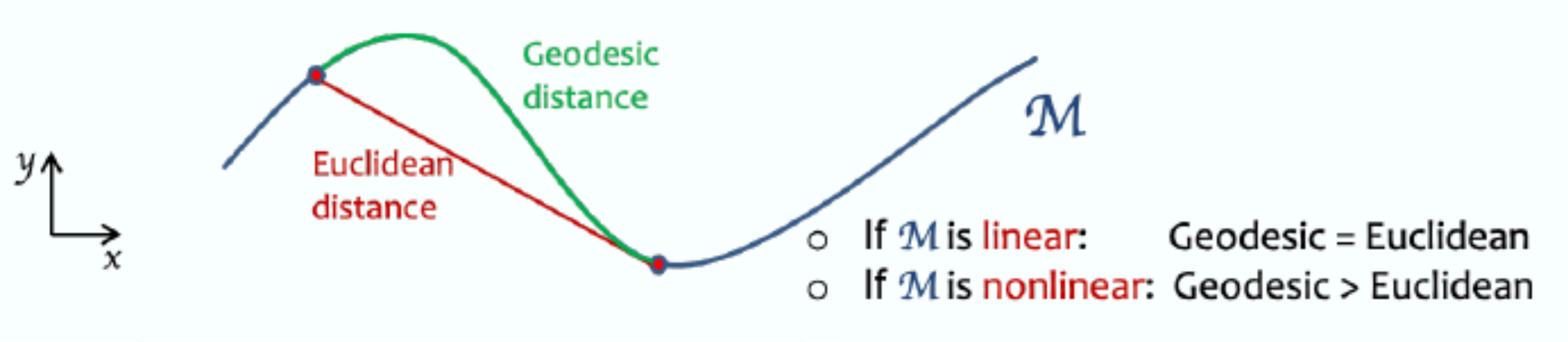

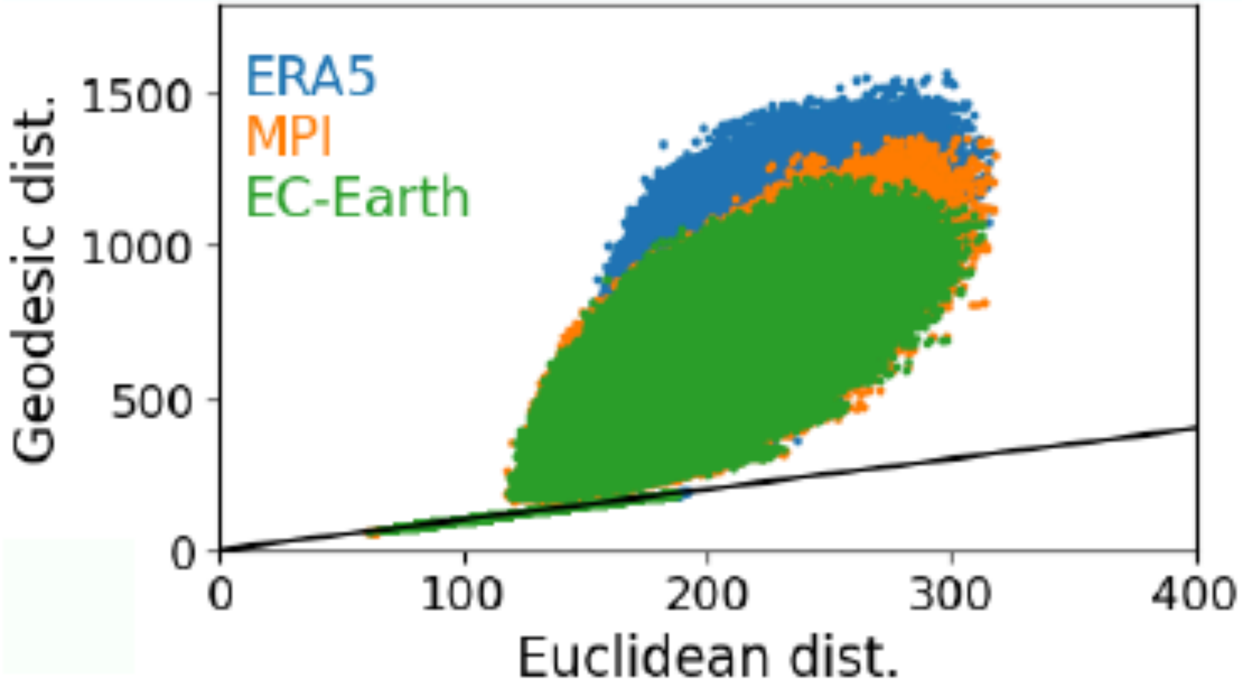

	Euclidean dist. μ±σ	Geodesic dist. μ±σ
Raw		
ERA5	123.4±16.0	425.9±122.0
MPI	124.5±20.4	445.2±145.5
EC-Earth	125.0±22.4	463.0±158.8
Anomalies		
ERA5	184.0±18.1	584.0±146.5
MPI	184.0±18.4	565.4±114.8
EC-Earth	184.1±17.2	549.4±106.0

PRESENT

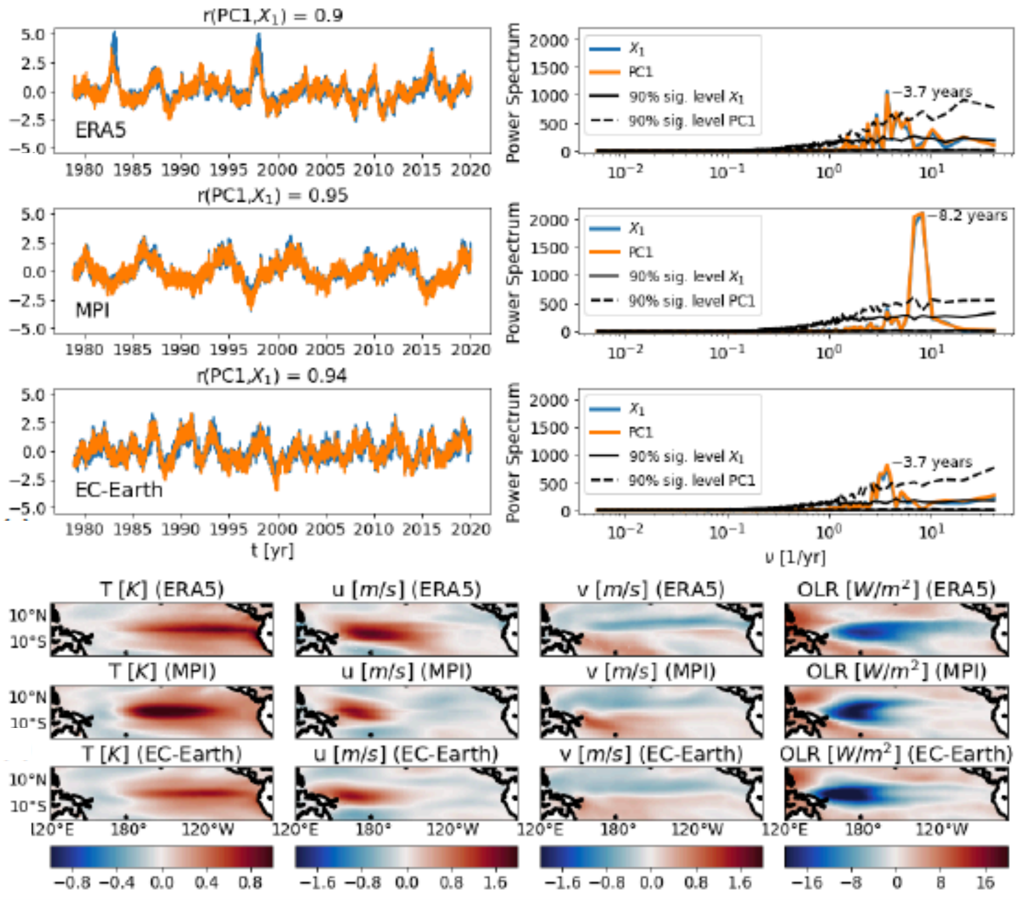

FUTURE

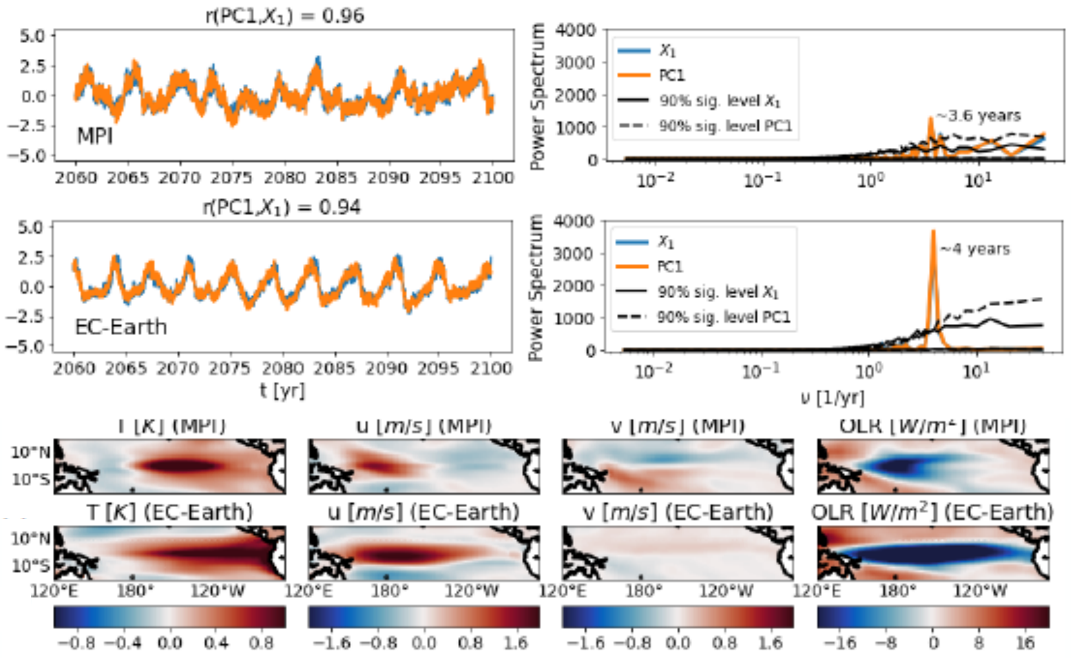

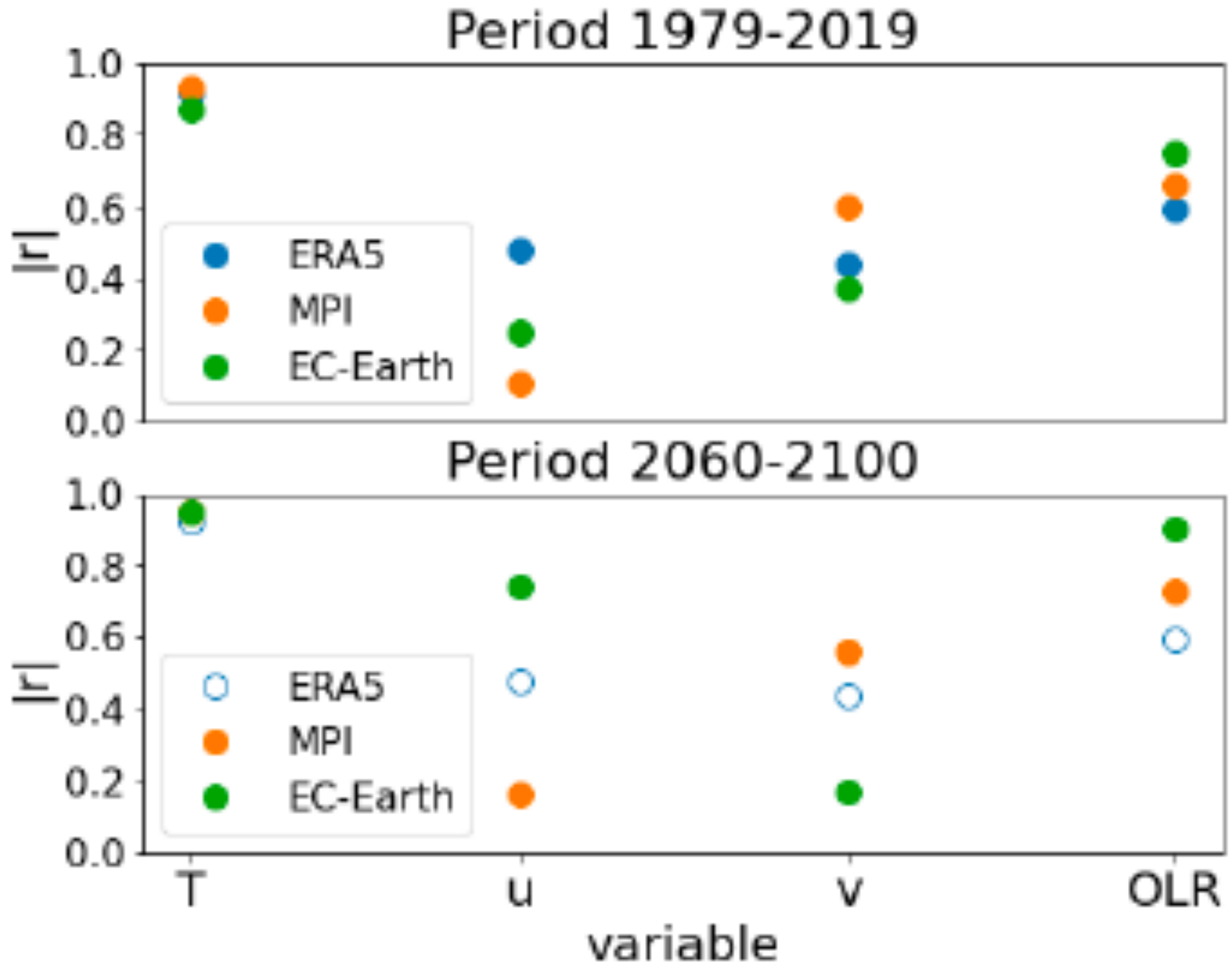

Correlations (in absolute value) between the first Isomap component of each variable (on the x-axis) and the multivariate case in ERA5 and models

Results: ENSO metrics

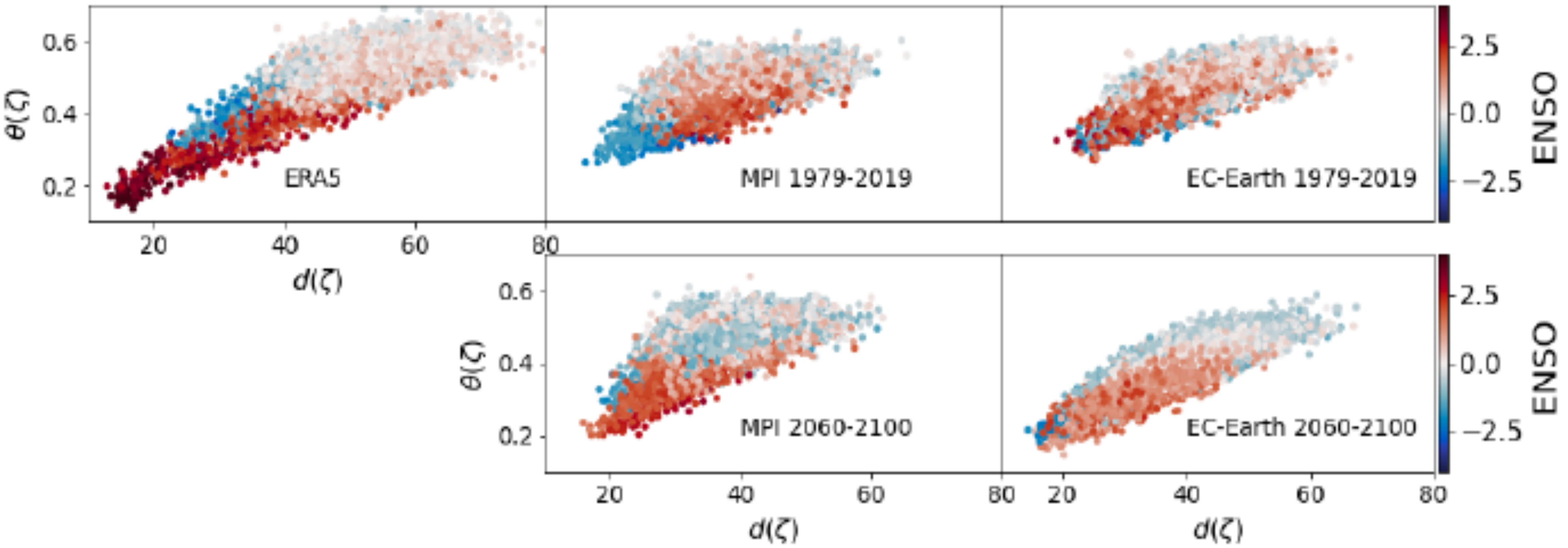

Results: ENSO metrics

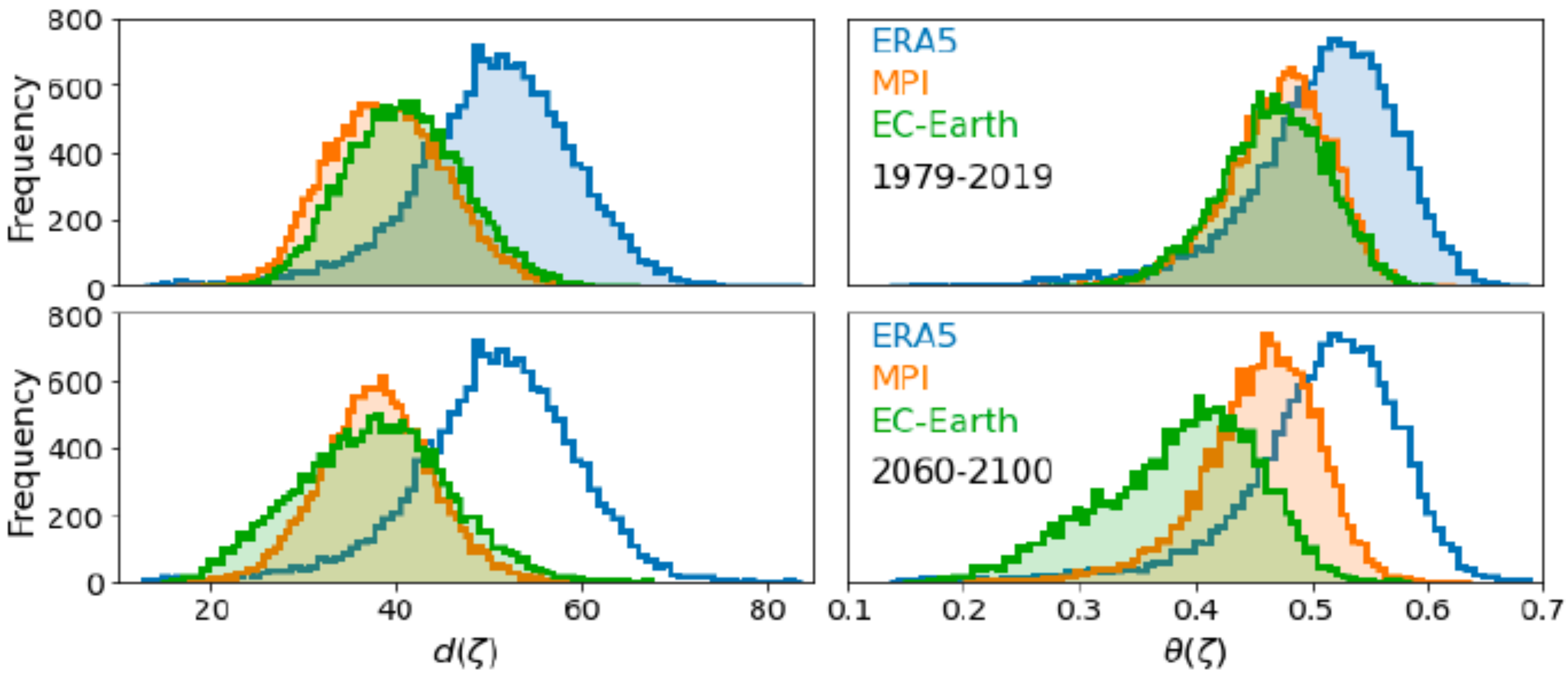

	μ_d	σ_d	γ_d	κ_d	μ_θ	σ_θ	γ_θ	κ_θ
Period 1979-2019								
ERA5	50.38	8.85	-0.59	4.21	0.51	0.07	-1.28	5.92
MPI	38.92	6.45	0.11	2.88	0.47	0.05	-0.58	3.65
EC-Earth	40.91	6.41	0.15	2.90	0.47	0.05	-0.32	3.10
Period 2060-2100								
MPI	37.89	5.98	0.06	3.19	0.45	0.05	-0.82	4.42
EC-Earth	37.33	8.02	0.07	2.76	0.38	0.07	-0.46	2.75

Results: ENSO metrics

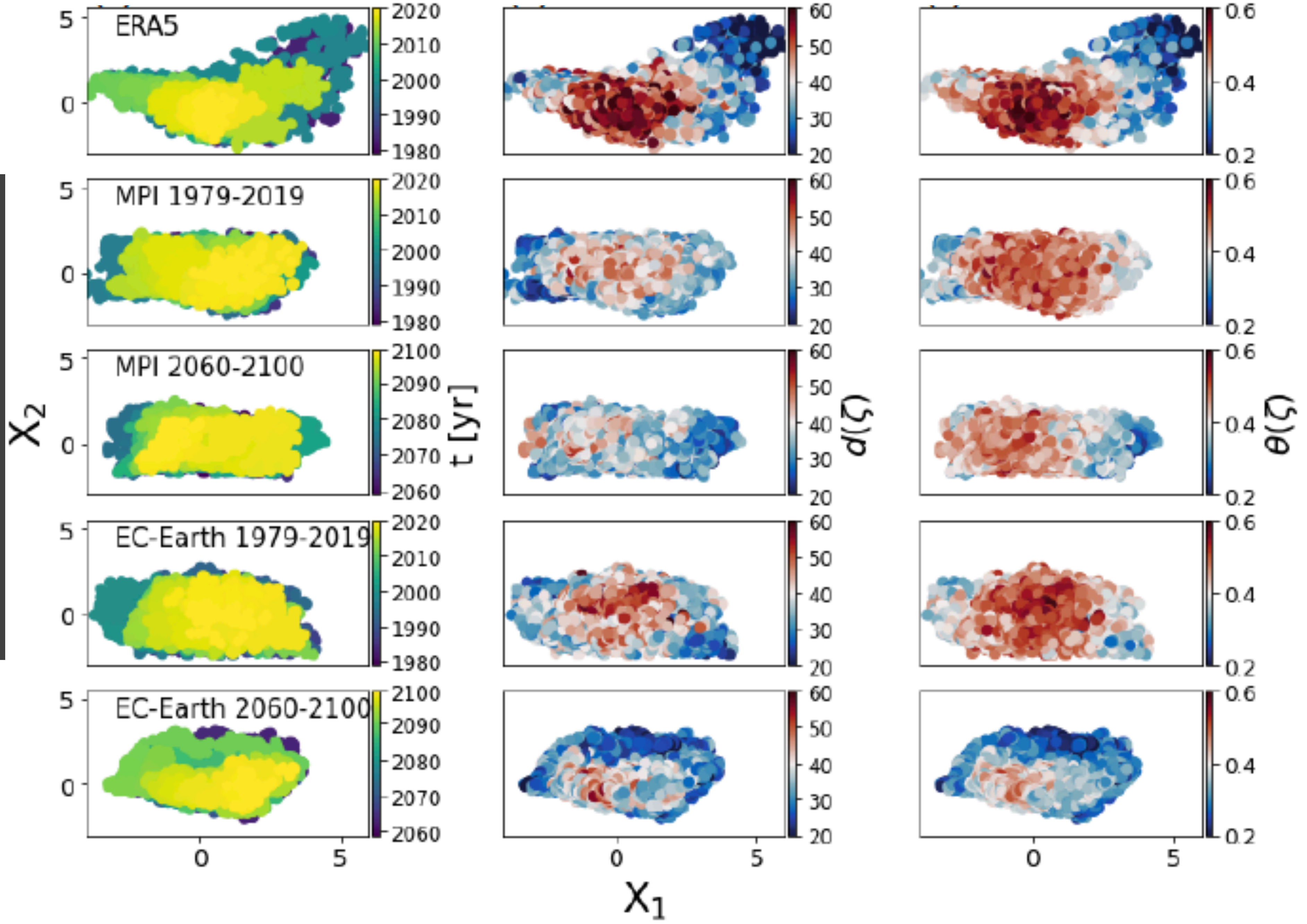

Conclusions

In ERA5 Isomap shows faster saturation of the residual variance compared to PCA → fewer dimensional components required for describing dynamics than for PCA. Not true for models

Models have different ENSO representations but manifolds share similar geometrical properties. True despite different resolutions and different parameterizations of unresolved processes.

The Isomap residual variance for variability part differs from PCA in the reanalysis but not so much in models → MPI and EC-Earth struggle in capturing the nonlinear topological characteristics of the observed manifold and they do so in a similar way

Conclusions

Under the SSP585 scenario, ENSO intensifies slightly in variance but does not change its spatial (biased) imprinting in MPI, while strongly intensifies in variance and displays a drastic change in the surface winds and OLR response in EC-Earth.

The three strongest global-scale El Nino events in the past 40 years explore a portion of the state space never visited in the model runs analyzed. At the same time, the local scale chaoticity of the deseasonalized, detrended anomalies remains badly underestimated, independently of model resolution.

Framework allows for:

- Quantifying how well links among variables are represented + their linear and nonlinear contributions
- Assessing the usefulness of stochastic perturbation schemes
- Developing machine learning applications based on the characterization of the global climate topology.